Synthesis, Characterization, and Reaction Chemistry of Complexes of the Molybdenum–Pentadienyl–Nitrogen Ligand System. Molecular Structure and Reactivity of 16-Electron *syn*-η^3-Pentadienyl Complexes

Shie-Fu Lush,[†] Shin-Hwan Wang,[†] Gene-Hsian Lee,[‡] Shie-Ming Peng,[‡] Sue-Lein Wang,[†] and Rai-Shung Liu*[,†]

Departments of Chemistry, National Tsing Hua University, Hsinchu, Taiwan, Republic of China, and National Taiwan University, Taipei, Taiwan, Republic of China

Received November 27, 1989

The reaction between $Mo(CO)_2(CH_3CN)_2(\eta^3\text{-}C_5H_7)Br$ and 2,2′-bipyridine (bpy) or 1,10-phenanthroline (phen) yields complexes of the type $Mo(CO)_2(N\frown N)(\eta^3\text{-}C_5H_7)Br$ ($N\frown N$ = bpy (**1a**), phen (**1b**)), respectively. Treatment of **1a** or **1b** with $AgBF_4$ in CH_2Cl_2 respectively gives $Mo(CO)_2(N\frown N)(\eta^3\text{-}C_5H_7)BF_4$ ($N\frown N$ = bpy (**2a**), phen (**2b**)), in which the pentadienyl ligand adopts a syn-η^3 configuration, whereas the BF_4^- anion serves as η^1-coordinating ligand. In donor solvents such as CH_3CN, THF, and acetone, **2a** and **2b** take up one solvent molecule to yield complexes of the type $[Mo(CO)_2(N\frown N)(\eta^3\text{-}C_5H_7)S]BF_4$ ($N\frown N$ = bpy, S = CH_3CN (**3a**), acetone (**3b**), ether (**3c**); $N\frown N$ = phen, S = CH_3CN (**4a**), acetone (**4b**), ether (**4c**)). For **3a** and **4a**, two conformers are isolable in equal proportions. A ^1H spin saturation transfer experiment reveals that the two isomers undergo mutual exchange by rotation of the metal–allyl bond. For **3b,c**, and **4b,c**, one extra pair of conformers was detected in addition to the isomers identical with those of **3a** and **4a**. The 16-electron compound $Mo(CO)_2(N\frown N)(\eta^3\text{-}C_5H_7)$ (**5a**; $N\frown N$ = $(C_6H_5)_2B(pz)_2$, pz = pyrazolyl) has been synthesized from the reaction between $NaB(C_6H_5)_2(pz)_2$ and $Mo(CO)_2(CH_3CN)_2(\eta^3\text{-}C_5H_7)Br$. The solid-state structure of **5a** has been fully characterized. In solution, the molecule is stereochemically nonrigid. There is NMR evidence that shows the chemical exchange between the two inequivalent pyrazole and the two inequivalent phenyl groups. The fluxional mechanism proceeds with rotation of the chelate nitrogen ligand along the Mo–B axis. Complex **5a** reacts with tertiary phosphines to produce the 18-electron complexes $Mo(CO)_2(N\frown N)(\eta^3\text{-}C_5H_7)L$ (L = PMe_3 (**6a**), $P(OPh)_3$ (**6b**)). The reaction between H_2O and **5a** gives $[(C_6H_5)_2B(pz)(OH)Mo(\eta^3\text{-}NNCHCHCHCH_2CHCHCHCH_3)]$ (**7a**) in moderate yield. Structural characterization of **7a** was achieved by X-ray diffraction studies of its tungsten analogue **7b**. Molecular structures of **3a**, **5a**, **6a**, and **7b** have been determined by X-ray diffraction with the following parameters: **3a**, space group $P\bar{1}$, a = 8.107 (4) Å, b = 11.055 (3) Å, c = 13.118 (3) Å, α = 106.42 (2)°, β = 95.39 (3)°, γ = 96.41 (3)°, R = 4.0% and R_w = 4.1% for 2624 reflections >3.0$\sigma(I)$; **5a**, space group $P\bar{1}$, a = 9.951 (13) Å, b = 10.435 (7) Å, c = 12.210 (8) Å, α = 82.31 (6)°, β = 79.27 (9)°, γ = 74.62 (10)°, R = 6.7%, and R_w = 7.4% for 2368 reflections >2.0$\sigma(I)$; **6a**, space group $P2_1/c$, a = 14.552 (5) Å, b = 9.7108 (23) Å, c = 19.862 (8) Å, β = 90.48 (3)°, Z = 4, R = 4.2% and R_w = 3.6% for 1421 reflections >2.0$\sigma(I)$; **7b**, space group $P2_12_12_1$, a = 10.0979 (21) Å, b = 13.6753 (23) Å, c = 17.331 (3) Å, Z = 4, R = 3.2% and R_w = 2.7%, for 2650 reflections >2.0$\sigma(I)$.

Introduction

Recently, transition-metal–pentadienyl complexes have been a subject of intensive study.[1,2] The chemical reactivity of η^5-pentadienyl complexes is particularly interesting. The η^5 ligand is capable of undergoing coupling reactions with metal or small molecules to form metal-coordinated metallabenzene[3] and 1,3,7,9-decatetraene–metal complexes[4] as well as an interesting [5 + 1] acetylation adduct.[5] Studies of electron-rich metal–η^5-pentadienyl–phosphine systems[6] have revealed that the metal center readily undergoes oxidation as well as electrophilic addition. Particularly notable are the metal–η^5-pentadienyl cations such as $(\eta^5\text{-dienyl})Fe(CO)_3^+$, which have been utilized extensively in organic reactions as well as natural product synthesis.[7]

Another interesting character of η^5-metal–pentadienyl complexes is the facile interconversion between the η^5 and η^3 bonding modes. In our previous papers,[8] we have reported an equilibrium between the cations $[(\eta^5\text{-}C_5H_7)Mo(CO)_2(P\frown P)]^+$ and $[(\eta^3\text{-}C_5H_7)Mo(CO)_2(CH_3CN)(P\frown P)]$ ($P\frown P$ = dmpe, dppe). Thermal parameters for the equilibrium $\eta^5\text{–}CH_3CN \rightleftarrows \eta^3 + CH_3CN$ calculated from equilibrium constants at various temperatures produced ΔH = 7–10 kcal mol^{-1} and ΔS = 28–32 cal mol^{-1} K^{-1}. These values reflect a delicate balance between the energetics of these two species. For the cyclopentadienyl counterpart, an equilibrium between the η^5 and η^3 modes has been observed in several systems; the ring-slippage nature of the ligand often leads to the occurrence of novel chemistry.[9] In order to clarify the key factors that determine the pentadienyl geometry in η^3 or η^5 forms, we turn to the synthesis of this class of compounds containing strong donor groups such as bipyridine or phenanthroline.

[†] National Tsing Hua University.
[‡] National Taiwan University.

(1) For review papers of acyclic metal–pentadienyl complexes, see: (a) Ernst, R. D. *Chem. Rev.* **1988**, *88*, 1251. (b) Ernst, R. D. *Acc. Chem. Res.* **1985**, *18*, 56. (c) Yasuda, H.; Nakamura, A. *J. Organomet. Chem.* **1985**, *285*, 15. (d) Powell, P. *Adv. Organomet. Chem.* **1986**, *26*, 125.

(2) (a) Bleeke, J. R.; Kotyk, J. *Organometallics* **1983**, *2*, 1263. (b) Bleeke, J. R.; Peng, W.-J. *Ibid.* **1987**, *6*, 1576. (c) Bleeke, J. R.; Hays, M. K.; Wittenbrink, R. J. *Ibid.* **1988**, *7*, 1417.

(3) Kralik, M. S.; Rheingold, A. L.; Ernst, R. D. *Organometallics* **1987**, *6*, 2612.

(4) (a) Bleeke, J. R.; Kotyk, J. J. *Organometallics* **1983**, *2*, 1263. (b) Wilson, D. R.; Ernst, R. D.; Kralik, M. S. *Ibid.* **1984**, *3*, 1442.

(5) Kralik, M. S.; Hutchinson, J. P.; Ernst, R. D. *J. Am. Chem. Soc.* **1985**, *107*, 8296.

(6) Bleeke, J. R.; Kotyk, J. J.; Moore, D. A.; Rauscher, D. J. *J. Am. Chem. Soc.* **1987**, *109*, 417.

(7) (a) Pearson, A. J. *Acc. Chem. Res.* **1980**, *13*, 463. (b) Kane-Maguire, L. A. P.; Honig, E. D.; Sweigart, D. A. *Chem. Rev.* **1984**, *84*, 525.

(8) Lee, G.-H.; Peng, S.-M.; Tsung, I.-C.; Mu, D.; Liu, R.-S. *Organometallics* **1989**, *8*, 2248.

(9) O'Connor, J. M.; Casey, C. P. *Chem. Rev.* **1987**, *87*, 308.

0276-7333/90/2309-1862$02.50/0

Results and Discussion

Synthesis of (η^3-pentadienyl)Mo(CO)$_2$(N⌒N)(η^1-BF$_4$). Mo(CO)$_2$(CH$_3$CN)$_2$(η^3-C$_3$H$_5$)Br[10] has been utilized very extensively as the synthetic precursor to complexes of the type Mo(CO)$_2$L$_2$(η^3-C$_3$H$_5$)Br because of the readily displacable acetonitrile molecules. For this reason, we first investigated the reaction of (η^3-pentadienyl)Mo(CO)$_2$(CH$_3$CN)$_2$Br[11] with bipyridine and phenanthroline.

Treatment of (η^3-pentadienyl)Mo(CO)$_2$(CH$_3$CN)$_2$Br with bipyridine or phenanthroline in CH_2Cl_2 at 0 °C yields (η^3-pentadienyl)Mo(CO)$_2$(N⌒N)Br (N⌒N = bpy (**1a**), phen (**1b**)) in high yield. Complexes **1a** and **1b** are deep red, air-sensitive crystalline solids that can be fully characterized spectroscopically. Elemental analyses are consistent with the given formulas. Solution IR spectra show the two carbonyls in equal intensity; this observation indicates that the two carbonyls are mutually cis. ^{1}H NMR spectra reveal that the ligand adopts a syn-η^3 geometry as indicated by the trans coupling pattern J_{34} = 10.0 Hz. In fact, the W-shaped syn geomtry is a common feature of most η^3-pentadienyl complexes:[12]

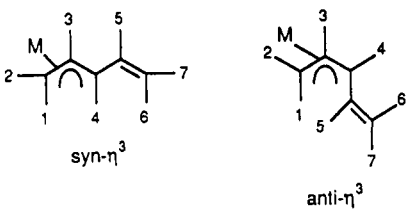

Treatment of **1a** and **1b** with 1.2 equiv of $AgBF_4$ in CH_2Cl_2 produced the air-sensitive solid (η^3-pentadienyl)Mo(CO)$_2$(N⌒N)(η^1-BF)$_4$ in high yield (N⌒N = bpy (**2a**), phen (**2b**)). Removal of halide ions from metal-η^3-pentadienyl complexes is known to be a general method to afford η^5-pentadienyl cations. The examples are (η^3-C$_5$H$_7$)M(CO)$_2$(P⌒P)Cl[8] (M = Mo, W; P⌒P = dppe, dmpe) and (η^3-C$_5$H$_7$)Ru(PMe$_3$)$_3$Cl.[13] Notably, the ligand geometry of **2a** and **2b** was identified as syn-η^3 rather than the expected η^5 cation. The two carbonyls absorb at 1948 (s) and 1868 (s) cm^{-1}, close to the absorptions for **1a** and **1b**. Previous studies on the [(η^5-C$_5$H$_7$)Mo(CO)$_2$(P⌒P)]$^+$ system have concluded that the η^5 cation is expected to have a 30–50-cm^{-1} increase in the ν(CO) absorption frequencies relative to those of **1a** and **1b**. In addition, a free ν(C=C) band is found at 1605 (w) cm^{-1}. The ^{1}H NMR spectra of **2a** and **2b** show that the pentadienyl proton resonances display the pattern of a syn-η^3 ligand. In order to satisfy the EAN rule, the BF_4^- anion probably acts as a ligating anion like those of CpMo(CO)$_3$(η^1-BF$_4$),[14] W(CO)$_3$NO(PR$_3$)(η^1-BF$_4$),[15] and others.[15] Characterization of the BF_4^- anion rests on the variable-temperature ^{19}F NMR spectra at −60 °C. The ^{19}F NMR spectrum of **2a** consists of a doublet at δ −148.2 ppm and a quartet at δ −144.2, assignable to the terminal and bridging fluorine atoms. The magnitude of the coupling constant $^2J_{FF}$, 88 Hz, is comparable to other published data.[15] At elevated temperatures, the two signals begin to broaden and coalesce to one signal at −146.8 ppm at 0 °C. A similar NMR pattern is also observed for **2a**. These NMR results reflect that the η^1 Mo–F–BF$_3$ bonding is weak and is readily cleaved at ambient temperature to allow the exchange of the terminal and bridging sites. $\Delta G^\ddagger$ values calculated from line-shape analysis of the spectra are 9.5 ± 0.3 and 9.6 ± 0.3 kcal mol^{-1} for **2a** and **2b**, respectively.

Scheme I

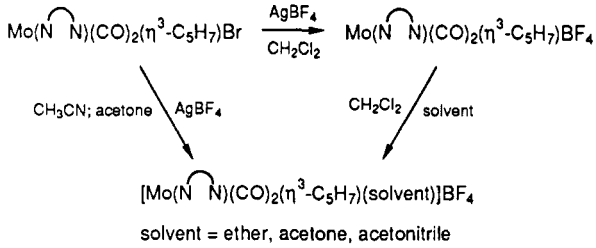

For "noncoordinating anions",[16] recent studies have shown that the order of ligand binding strength is $SbF_6^- > BF_4^- > PF_6^-$. We have prepared the PF_6^- salt of **2b** to examine its pentadienyl ligand structure. In solid form, the complex is less stable than the BF_4^- salt and decomposes within 2 days. The IR spectra in either Nujol mull or CH_2Cl_2 solution all show the presence of a free ν(C=C) band at 1605 (m) cm^{-1}. The ^{1}H NMR spectra in CD_2Cl_2 revealed a pattern with that identical for the BF_4^- salt. The ^{19}F NMR spectra showed an ill-defined broad line at −80 °C, which became a doublet at −40 °C (J_{PF} = 290 Hz). These spectroscopic data suggest that PF_6^-, like BF_4^-, acts as a coordinating ligand to achieve 18-electron status.

Synthesis of [(η^3-pentadienyl)Mo(CO)$_2$(N⌒N)(solvent)]BF$_4$. The η^1-bound BF_4^- and PF_6^- anions are readily displaced by donor solvents. As depicted in Scheme I, addition of excess ligating solvents to dichloromethane solutions of **2a** and **2b** produced air-stable red crystals formulated as [(η^3-pentadienyl)Mo(CO)$_2$(N⌒N)S]BF$_4$ (N⌒N = bpy, S = CH$_3$CN (**3a**), acetone (**3b**), ether (**3c**); N⌒N = phenanthroline, S = CH$_3$CN (**4a**), acetone (**4b**), ether (**4c**)). Alternative synthesis of **3a**, **4a** and **3b**, **4b** involves the reaction between $AgBF_4$ and **1a** or **1b** in the mother solvents. For **3a** and **4a**, two conformers are recognizable from their NMR spectra. Their structural variations arise from the different orientations of the pentadienyl group (exo or endo) with respect to the coordinated CH$_3$CN molecule. This exo–endo assignment is confirmed by a proton spin-transfer experiment as well as by X-ray diffraction of **3a** (vide infra). Figure 1a depicts the NMR spectrum of the two conformers, and the assignment of pentadienyl proton signals is based on COSY-2D NMR spectra. Irradiation of the H^3 signal of the major isomer at δ 4.38 ppm leads to disappearance of the H^3 signal of the minor isomer at 3.55 ppm, whereas the other proton resonances remain with the same intensity. A similar site exchange is observed for the H^6 signals of the two isomers at δ 6.52 and 5.48 ppm in a spin-transfer experiment. For the other protons, because of the very close chemical shifts, irradiation of the H^i signal expectedly results in disappearance of the corresponding proton signal of the other isomer; nevertheless, the signals of the other protons remain with the same intensity. These results are sufficient to establish the following site exchanges H^1 ⇄ H$^{1'}$, H^2 ⇄ H$^{2'}$, H^3 ⇄ H$^{3'}$. In contrast, the bipyridine group

(10) (a) Brisdon, B. J. *J. Organomet. Chem.* **1977**, *125*, 225. (b) Faller, J. W.; Haitko, D. A.; Adams, R. D.; Chodosh, D. F. *J. Am. Chem. Soc.* **1979**, *101*, 865.
(11) Lee, G.-H.; Peng, S.-M.; Liu, F.-C.; Liu, R.-S. *Organometallics* **1989**, *8*, 402.
(12) (a) Lee, T. W.; Liu, R.-S. *Organometallics* **1988**, *7*, 878. (b) Lee, G.-H.; Peng, S.-M.; Lush, S.-F.; Liu, R.-S. *Ibid.* **1987**, *6*, 2094. (c) Lee, G.-H.; Peng, S.-M.; Liao, M. Y.; Liu, R.-S. *J. Organomet. Chem.* **1986**, *312*, 113.
(13) Bleeke, J. R.; Rauscher, D. J. *Organometallics*, **1988**, *7*, 2328.
(14) Sunkel, K.; Nagel, V.; Beck, W. *J. Organomet. Chem.* **1983**, *251*, 227.
(15) Honeychuck, R. V.; Hersh, W. H. *Inorg. Chem.* **1989**, *28*, 2869.
(16) For other related cations, only the complex [(bpy)Mo(CO)$_2$(η^3-C$_3$H$_5$)(pyridine)]$^+$ has been reported; see: Fenn, R. H.; Graham, A. J. *J. Organomet. Chem.* **1972**, *37*, 137.

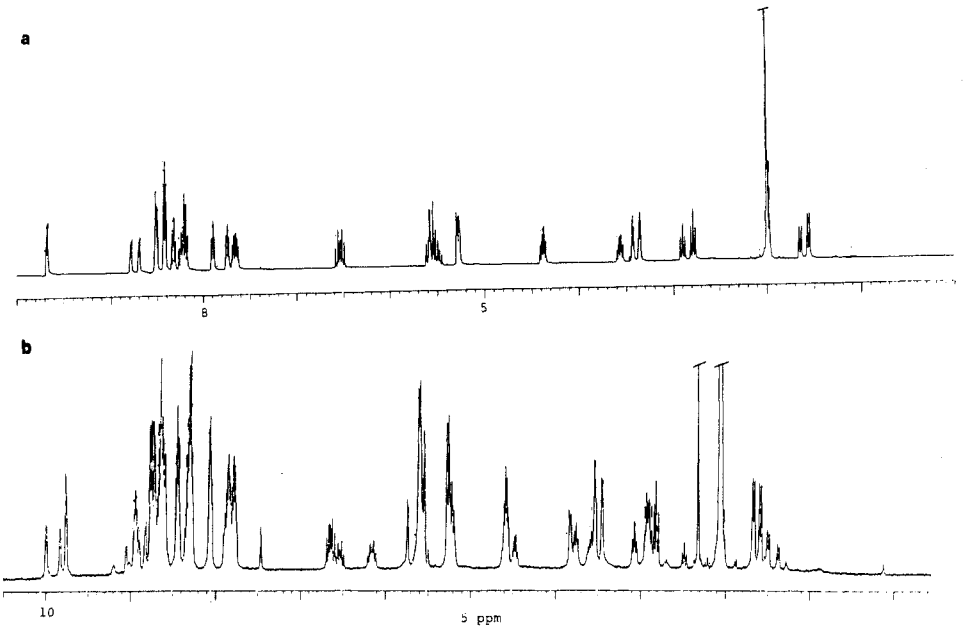

Figure 1. ^1H NMR spectra of (a) **3a** in CD_3CN and (b) **3b** in CD_3COCD_3.

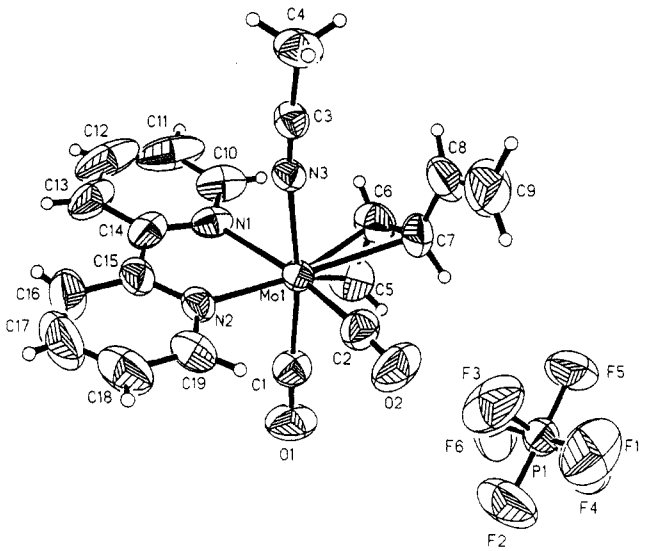

Figure 2. ORTEP drawing of **3a**.

appears to be stereochemically rigid. Figure 1a depicts the 16 inequivalent signals of the bipyridine protons of the two isomers in the low-field δ 7.5–9.5 ppm region. Irradiation of the signal at δ 9.65 ppm shows no sign of decrease in the intensity of the other protons. The results above lead to a conclusion that the two stereoisomers undergo an exchange mechanism involving a pseudorotation along the Mo···allyl axis.

Because the corresponding allyl cations $[(N\frown N)Mo(CO)_2(\eta^3\text{-}C_3H_5)S]^+$ (S = CH_3CN, THF, acetone) still remain unknown,[16] we have performed an X-ray diffraction study of **3a** to elucidate the solid-state structure. We substituted the counterion PF_6^- for BF_4^- to achieve better crystal quality. The ORTEP drawing is given in Figure 2; selected bond distances and angles are given in Table I. The coordination geometry around the molybdenum atom is approximately an octahedron with the two bipyridine nitrogens, acetonitrile, two carbonyls, and the allyl group occupying the six coordination sites. Stereochemically, the two nitrogen atoms, N1 and N2 lie trans to the acetonitrile and pentadienyl groups, respectively. Because of the steric effect of the large allyl group, the CH_3CN ligand tilts toward the pyridine group with the bond angles N1–Mo–N3 = 79.8 (2)° and N2–Mo–N3 = 82.2 (3)°. The pentadienyl group is planar with a dihedral angle of 3.2° between the vinylic plane C7–C8–C9 and the allylis plane C5–C6–C7. The pentadienyl group assumes a W-shaped configuration that has a staggered orientation with respect to the N2–C1–C2 face; i.e., the mouth of the allyl group faces the two carbonyls. The pentadienyl carbon atoms C5, C6, C7, and C8 are essentially coplanar, whereas C9 lies 0.082 Å out of the plane and toward the molybdenum atom. The torsional angle C5–C6–C7–C8 is −176.2°.

Table I. Bond Lengths (Å) and Bond Angles (deg) for 3a

Mo1–N1	2.276 (5)	Mo1–N2	2.203 (5)
Mo1–N3	2.227 (4)	Mo1–C1	1.961 (6)
Mo1–C2	1.949 (7)	Mo1–C5	2.301 (9)
Mo1–C6	2.232 (8)	Mo1–C7	2.422 (8)
O1–C1	1.144 (7)	O2–C2	1.159 (8)
N3–C3	1.134 (7)	C3–C4	1.443 (9)
C5–C6	1.403 (11)	C6–C7	1.372 (12)
C7–C8	1.467 (11)	C8–C9	1.290 (18)
N1–Mo1–N2	72.7 (2)	N1–Mo1–N3	79.8 (2)
N2–Mo1–N3	82.3 (2)	N1–Mo1–C1	100.9 (2)
N2–Mo1–C1	85.8 (2)	N3–Mo1–C1	167.3 (2)
N1–Mo1–C2	166.5 (3)	N2–Mo1–C2	94.0 (2)
N3–Mo1–C2	96.7 (2)	C1–Mo1–C2	79.7 (3)
N1–Mo1–C5	86.8 (2)	N2–Mo1–C5	144.5 (3)
N3–Mo1–C5	123.1 (2)	C1–Mo1–C5	69.6 (3)
C2–Mo1–C5	105.8 (3)	N1–Mo1–C6	91.5 (3)
N2–Mo1–C6	163.0 (2)	N3–Mo1–C6	89.0 (2)
C1–Mo1–C6	103.7 (3)	C2–Mo1–C6	101.6 (3)
C5–Mo1–C6	36.0 (3)	N1–Mo1–C7	122.1 (2)
N2–Mo1–C7	155.3 (2)	N3–Mo1–C7	81.5 (2)
C1–Mo1–C7	108.2 (3)	C2–Mo1–C7	69.7 (3)
C5–Mo1–C7	60.0 (3)	C6–Mo1–C7	34.0 (3)
Mo1–N1–C10	125.1 (5)	C10–N1–C14	118.6 (6)
Mo1–N2–C19	122.5 (4)	Mo1–N3–C3	173.0 (5)
Mo1–C1–O1	176.0 (6)	Mo1–C2–O2	176.0 (6)
N3–C3–C4	177.8 (7)	Mo1–C5–C6	69.3 (5)
Mo1–C6–C5	74.7 (5)	Mo1–C6–C7	80.6 (5)
C5–C6–C7	117.0 (6)	Mo1–C7–C6	65.4 (5)
Mo1–C7–C8	118.3 (6)	C7–C8–C9	125.4 (8)

For complexes **3b,c** and **4b,c**, four stereoisomers are detectable in high-field ^1H NMR spectra. Figure 1b displays the ^1H NMR spectrum of **3b**, which reveals the four stereoisomers with the pentadienyl ligand in syn-η^3 configurations. The assignment of NMR signals to the pentadienyl protons is based on 2D-COSY NMR spectra. Notably, the two major isomers with the H^1 proton reso-

nances at δ 1.60 and 1.80 ppm have structures identical with those of **3a** and **4a** upon comparison of the NMR data. Likewise, the two new isomers exist as exo–endo conformers due to the different pentadienyl orientations relative to the $[Mo(N\frown N)(CO)_2S]^+$ fragment. This structural assignment has been proved by a proton spin-transfer experiment as previously described for **3a** and **3b**. Irradiation of the H^4 signal at δ 2.50 ppm causes the disappearance of the H^4 signal at δ 3.08 ppm, whereas the H^4 signals at δ 2.82 and 2.90 ppm of the major isomers retain the same intensity. Irradiation of the H^5 signal at δ 6.15 ppm results in disappearance of the H^5 signals at δ 6.50 ppm, whereas the H^5 signals at δ 6.65 and 5.50 ppm of the major isomers retain the same intensity. This information indicates that complex **3b** exists as two geometric isomers and each geometric isomer consists of two exo–endo conformers. A similar observation applies to **3c** and **4b,c**, whose four stereoisomers are identical with those of **3b** on the basis of a comparison of their NMR data.

This work follows our previous studies involving the cations[8] $[(\eta^5\text{-}C_5H_7)Mo(CO)_2(P\frown P)]^+$ and $[(syn\text{-}\eta^3\text{-}C_5H_7)Mo(CO)_2(P\frown P)(CH_3CN)]^+$. These two cations are in equilibrium in CH_2Cl_2 and acetone solutions. In sharp contrast to the diphos group, the pentadienyl group of complexes of the type $(\eta^3\text{-}C_5H_7)Mo(CO)_2(N\frown N)L$ remains in the syn-η^3 configuration even though L herein is recognizable as a very weakly coordinating ligand. In our previous results,[11] we have shown the strength of the electron-accepting property of the pentadienyl group in complexes of the type $[(\eta^5\text{-}C_5H_7)Mo(CO)_2(P\frown P)]^+$. The ν(CO) band of the latter shows an increase in wavenumber of 30–50 cm^{-1} relative to that of the cation $[(\eta^3\text{-}C_5H_7)Mo(CO)_2(P\frown P)(CH_3CN)^+$. In principle, strong electron donors such as bipyridine and pyridine are expected to stabilize the η^5 cation because of their enhancement of metal electron density. In order to find a reasonable explanation, we examined interligand steric hindrance within the complex. In the $(\eta^5\text{-}C_5H_7)ML_4$ system,[6,17] all the known structures adopt conformation A. This structure is consistent with an early theoretical prediction;[18] notably, the distances of the Mo(II) ion to the pyridine nitrogen atom in complex **3a** are about 2.2–2.3 Å, which are shorter than the Mo–P distances (2.5–2.6 Å) in the complex $(\eta^5\text{-}C_5H_7)Mo(CO)_2(P\frown P)$. Structure B depicts a distorted-square-pyramidal structure, in which bipyridine replaces the diphos ligand. Because of the inflexibility of the pyridine group, the interligand steric hindrance between the dienyl group and the π-electrons of the bipyridine appears to be more severe than in the case of the diphos system. In this manner, the delicate $\eta^5 \rightleftarrows \eta^3$ balance in the diphos complexes is expected to shift toward the η^3 direction.

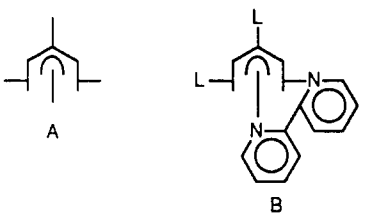

Synthesis and Structure of 16-Electron $[(C_6H_5)_2B(pz)_2Mo(CO)_2(syn\text{-}\eta^3\text{-}C_5H_7)]$. Sixteen-electron pentadienyl complexes such as $Cr[\eta^5\text{-}2,4\text{-}(CH_3)_2C_5H_5]_2$,[19] $(C_5H_5)Ti(2,4\text{-}C_5H_7)(PEt_3)$,[20] and $Cr(\eta^5\text{-}C_5H_7)[\eta^5\text{-}2,4\text{-}(CH_3)_2C_5H_5]$[21] are commonly known as open-sandwich complexes. Recently, $Rh(PR_3)_2[\eta^3\text{-}2,4\text{-}(CH_3)_2C_5H_5)]_2$ and $Rh(\eta^3\text{-}syn\text{-}C_5H_7)(pinacop)$[21] have been prepared. The latter has a 16-electron configuration, which is in fact a common feature of d^8 square-planar complexes. If the interligand steric hindrance is a key factor in the complex geometry of $[(\eta^3\text{-}C_5H_7)Mo(N\frown N)(CO)_2S]^+$, because of the very lability of S (S = CH_3CN, THF, acetone, BF_4^-), it is possible to prepare d^4 16-electron metal-*syn*-η^3-pentadienyl complexes in the presence of sterically demanding nitrogen groups such as $(C_6H_5)_2B(pz)_2^-$ (pz = pyrazolyl).

The reaction between $Na(C_6H_5)_2B(pz)_2$ and $Mo(CO)_2(CH_3CN)_2(\eta^3\text{-}C_5H_7)Br$ in dichloromethane solution produced $Mo(CO)_2(\eta^3\text{-}C_5H_7)(Ph_2B(pz)_2)$ (**5a**) in moderate yield. Complex **5a** was obtained as air-stable yellow crystals, the solid-state structure of which has been fully characterized by X-ray diffraction. An ORTEP drawing is shown in Figure 3; selected bond lengths and angles are given in Table II. The coordination geometry about the

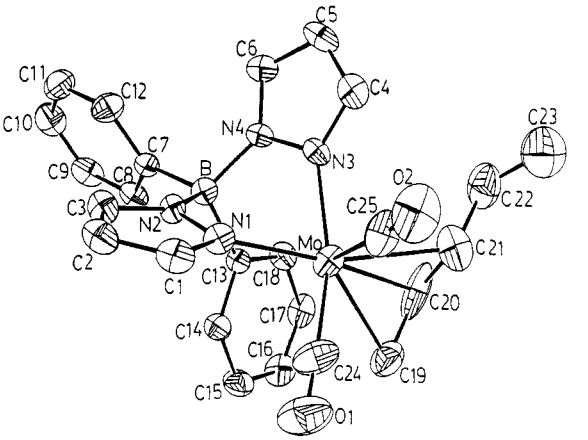

Figure 3. ORTEP drawing of **5a**.

Table II. Selected Bond Distances (Å) and Angles (deg) for 5a

Mo–N1	2.143 (9)	Mo–N3	2.172 (9)
Mo–C19	2.305 (12)	Mo–C20	2.210 (12)
Mo–C21	2.447 (15)	Mo–C24	1.952 (15)
Mo–C25	1.899 (13)	C13–B	1.616 (16)
N2–B	1.589 (14)	N4–B	1.547 (17)
C7–B	1.585 (16)	C20–C21	1.336 (22)
C21–C22	1.369 (23)	C22–C23	1.40 (3)
C24–O1	1.180 (18)	C25–O2	1.159 (15)
N1–Mo–N3	79.3 (3)	N1–Mo–C19	136.3 (5)
N1–Mo–C20	162.7 (4)	N1–Mo–C21	161.4 (4)
N1–Mo–C24	83.9 (5)	N1–Mo–C25	98.1 (5)
N3–Mo–C19	133.4 (5)	N3–Mo–C20	98.9 (5)
N3–Mo–C21	88.0 (4)	N3–Mo–C24	162.0 (5)
N3–Mo–C25	94.9 (5)	C19–Mo–C20	37.2 (7)
C19–Mo–C21	61.9 (5)	C19–Mo–C24	64.4 (6)
C19–Mo–C25	105.1 (5)	C20–Mo–C21	32.8 (5)
C20–Mo–C24	99.1 (6)	C20–Mo–C25	99.2 (6)
C21–Mo–C24	106.6 (6)	C21–Mo–C25	69.4 (5)
C24–Mo–C25	80.8 (6)	C19–C20–C21	123.4 (14)
C20–C21–C22	123.9 (14)	C21–C22–C23	119.6 (16)
Mo–C24–O1	173.8 (12)	Mo–C25–O2	177.3 (11)
N2–B–N4	104.6 (9)	N2–B–C7	108.8 (9)
N2–B–C13	105.5 (8)	N4–B–C7	112.0 (9)
N4–B–C13	110.4 (9)	C7–B–C13	114.8 (10)

(17) (a) Baudry, D.; Ephritikhine, M.; Felkin, H.; Jeannin, Y.; Robert, F. *J. Organomet. Chem.* **1981**, *220*, C7. (b) Waldman, T.; Rheingold, A. L.; Ernst, R. D. Unpublished results.
(18) Albright, T. A.; Hoffman, R.; Tse, Y.-C.; D'Ottavio, T. *J. Am. Chem. Soc.* **1979**, *101*, 3812.
(19) Newbound, T. D.; Freeman, J. W.; Wilson, D. R.; Kralik, M. S.; Patton, A. T.; Campana, C. F.; Ernst, R. D. *Organometallics* **1987**, *6*, 2432.
(20) Freeman, J. W.; Arif, A. M.; Ernst, R. D. Unpublished results.
(21) Melendez, E.; Arif, A. M.; Ziegler, M. L.; Ernst, R. D. *Angew. Chem., Int. Ed. Engl.* **1988**, *27*, 1099.
(22) Bleeke, J. R.; Donaldson, A. J.; Peng, W. J. *Organometallics* **1988**, *7*, 33.

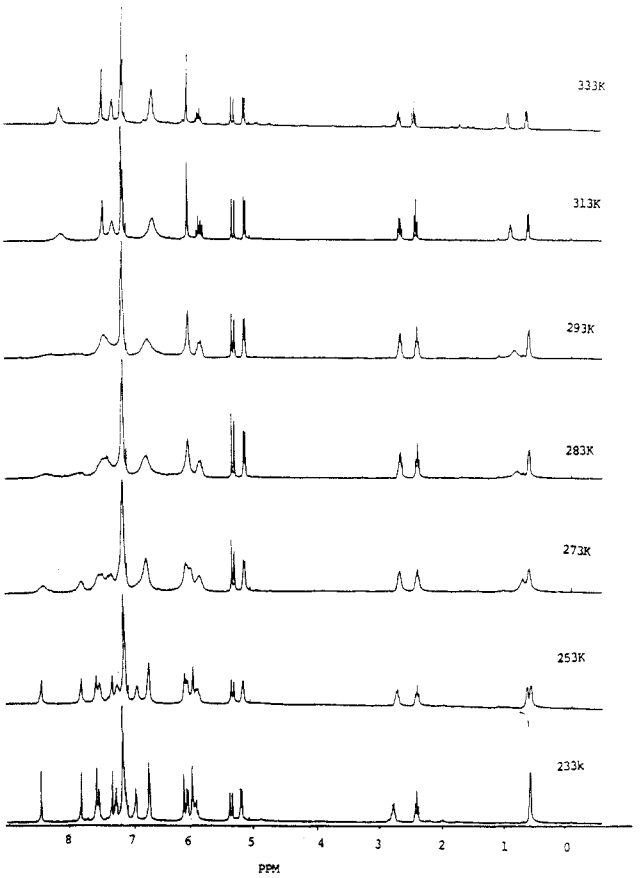

Figure 4. Variable-temperature ^1H NMR spectra of **5a** in toluene-d_8.

molybdenum atom is approximately square pyramidal with the atoms N1, N3, and C24 and an allyl group occupying the four basal sites and the C25–O2 bond occupying the apical site. The chelate ring is buckled into a boat conformation with the two pyrazole planes tilted toward the C25–O2 bond. The Mo···B distance is 3.226 (12) Å, similar to that for $[(pz)_2B(pz)_2Mo(CO)_2(\eta^3\text{-}2\text{-}(CH_3)C_3H_4)]$ (3.24 Å)[23] but far smaller than for $(C_2H_5)_2B(pz)_2(CO)_2(\eta^3\text{-}C_3H_5)Mo(C_3N_2H_4)$ (3.8 Å).[24] Apparently, there is no agostic Mo···H–C interaction between Mo and the ortho hydrogen of the phenyl group. The agostic Mo···H–C interaction has been known for complexes of the type $(R_2B(pz)_2)Mo(CO)_2(\eta^3\text{-}C_3H_5)$.[25] Particularly notable is the orientation of the two phenyl groups. One lies in the plane bisecting the two pyrazole groups to minimize steric hindrance, whereas the other phenyl group faces the molybdenum atom. This conformational structure is quite different from that of $[(C_6H_5)_2B(pz)_2Mo(CO)_2(\eta^3\text{-}C_5H_7)\text{-}PMe_3$, in which the two phenyl groups lie away from the metal center (vide infra). It is likely that there is a weak interaction between the molybdenum atom and π-electron density of the phenyl group in the vicinity of carbon atoms C13, C14, C15, and C16. Among them, the smallest Mo–C(14) distance is 3.158 (12) Å, which may indicate some weak donation of π-electron density to the molybdenum atom. The pentadienyl group has a W-shaped configuration, and the allyl mouth faces the apical C25–O2 group. A delocalization pattern in the pentadienyl bond length is evident; the observed C–C bond distances 1.33–1.44 Å

Scheme II

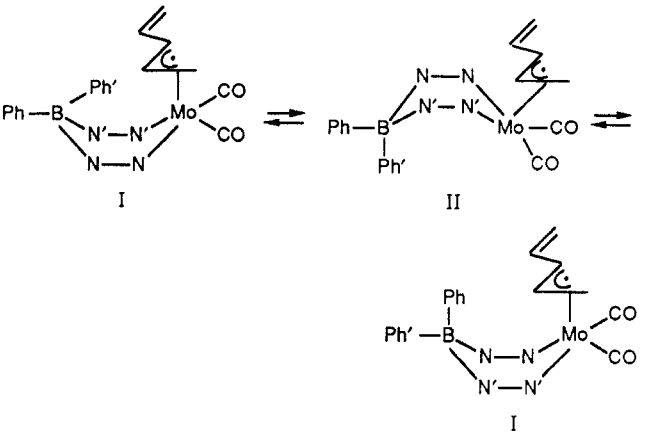

are intermediate between values for double and single bonds. The bond length C21–C22 (1.388 (17) Å) is comparable to that of the vinyl bond C22–C23 (1.40 (3) Å). This delocalized pattern has been observed for Mo(*anti*-η^3-C_5H_7)$(CO)_2$(dppe)Br[11] and Rh(η^3-*syn*-C_5H_7)(pinacop).[22] The pentadienyl carbon atoms C19–C20–C21 and C22 are quite planar, whereas C23 lies 0.42 (4) Å out of the plane and away from the molybdenum atom. The dihedral angle between the planes C19–C20–C21 and C21–C22–C23 is 17.8 (24)°.

Complex **5a** in solution exhibits fluxional behavior, and the dynamic process has been examined by variable-temperature ^1H and ^{13}C NMR spectra. As depicted in Figure 4, the ^1H NMR spectra in $CDCl_3$ at −60 °C are consistent with the solid-state structure, which exhibits two inequivalent pyrazole groups and two inequivalent phenyl groups. The ^1H NMR spectra are in accord with the ^{13}C NMR spectra at −60 °C, which additionally show that the two carbonyl groups are also inequivalent. When the temperature is increased from −60 to 80 °C, the resonances of the two pyrazole groups broaden and coalesce at 40 °C. A similar coalescence behavior is observed for the two phenyl groups. In contrast, the resonances of the pentadienyl group remain unchanged at the elevated temperatures. In the ^{13}C NMR spectra, an exchange process is indeed observed for the two phenyl groups as well as the two pyrazole groups; nevertheless, the two carbonyls still remain inequivalent at the elevated temperatures. These NMR data preclude an interconversion between the two enantiomers as known for the related complex $[Et_2B(pz)_2]Mo(CO)_2(\eta^3\text{-}C_3H_5)$.[25] A proper mechanism is proposed by Scheme II based on the NMR data. The process is initiated by rotation of the boat BNNMoNN geometry along the Mo–B axis by 180° with respect to the Mo$(CO)_2(\eta^3\text{-}C_5H_7)$ fragment, which generates the intermediate II. A flip of the boat conformation of II regenerates I, which in turn exchanges the two pyrazole groups and the axial–equatorial phenyl groups. Following this process, the two carbonyl resonances and the seven signals of the pentadienyl protons still remain inequivalent. This rotation mechanism has been previously described for the fluxional behavior of $CpMo(CO)_2(R_2B(pz)_2)$[26] and other related complexes.[26] Line-shaped analysis calculated from ^1H NMR spectra yields a value of 17.4 ± 0.4 kcal mol^{-1} for ΔG^*.

Reactivity of 5a. Complex **5a** has a 16-electron configuration that readily undergoes nucleophilic addition

(23) Cotton, F. A.; Frenz, B. A.; Murillo, C. A. *J. Am. Chem. Soc.* **1975**, *97*, 2118.
(24) Calderon, J. L.; Cotton, F. A.; Shaver, A. *J. Organomet. Chem.* **1972**, *42*, 419.
(25) Cotton, F. A.; Stanislowski, A. G. *J. Am. Chem. Soc.* **1974**, *96*, 5074.
(26) Calderon, J. L.; Cotton, F. A.; Shaver, A. *J. Organomet. Chem.* **1972**, *37*, 127.

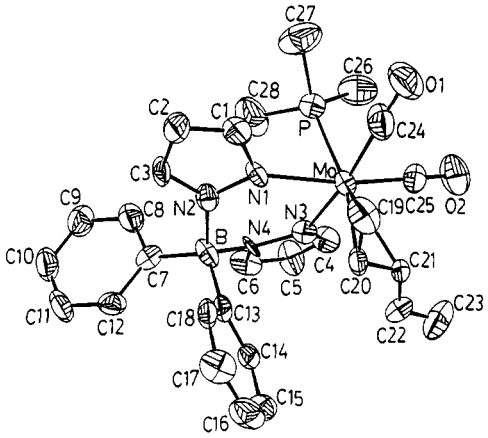

Figure 5. ORTEP drawing of **6a**.

Table III. Selected Bond Distances (Å) and Angles (deg) for 6a

Mo-P	2.540 (4)	Mo-N1	2.251 (8)
Mo-N3	2.250 (8)	Mo-C19	2.316 (12)
Mo-C20	2.218 (10)	Mo-C21	2.455 (11)
Mo-C24	1.900 (12)	Mo-C25	1.937 (10)
N1-N2	1.386 (11)	N1-C1	1.360 (13)
N2-C3	1.325 (13)	N2-B	1.570 (15)
N3-N4	1.384 (10)	C19-C20	1.357 (16)
N3-C4	1.328 (12)	C20-C21	1.390 (14)
N4-C6	1.358 (12)	C21-C22	1.419 (16)
N4-B	1.585 (14)	C22-C23	1.288 (17)
C7-B	1.608 (16)	C24-O1	1.171 (14)
C13-B	1.609 (17)	C25-O2	1.152 (12)
P-Mo-N1	81.08 (22)	P-Mo-N3	80.43 (24)
P-Mo-C19	145.8 (3)	P-Mo-C20	168.16 (25)
P-Mo-C21	153.1 (3)	P-Mo-C24	84.0 (4)
P-Mo-C25	89.0 (3)	N1-Mo-N3	84.2 (3)
N1-Mo-C19	80.3 (4)	N1-Mo-C20	88.3 (3)
N1-Mo-C21	120.3 (3)	N1-Mo-C24	97.4 (4)
N1-Mo-C25	169.9 (4)	N3-Mo-C19	125.6 (4)
N3-Mo-C20	93.4 (4)	N3-Mo-C21	85.5 (3)
N3-Mo-C24	163.9 (4)	N3-Mo-C25	96.2 (4)
C19-Mo-C20	34.7 (4)	C19-Mo-C21	59.8 (4)
C19-Mo-C24	70.3 (5)	C19-Mo-C25	107.3 (4)
C20-Mo-C21	34.1 (3)	C20-Mo-C24	102.6 (5)
C20-Mo-C25	101.7 (4)	C21-Mo-C24	107.1 (4)
C21-Mo-C25	69.7 (4)	C24-Mo-C25	79.5 (5)
C19-C20-C21	120.3 (9)	C20-C21-C22	128.1 (9)
C21-C22-C23	125.3 (11)	Mo-C24-O1	176.7 (10)
Mo-C25-O2	177.8 (10)	N2-B-N4	108.7 (8)
N2-B-C7	107.3 (9)	N2-B-C13	108.9 (9)
N4-B-C7	107.9 (9)	N4-B-C13	109.4 (9)
C7-B-C13	114.5 (8)		

with 1 equiv of tertiary phosphine in CH_2Cl_2 to produce air-stable red crystals formulated as $[(C_6H_5)_2B(pz)_2]Mo(CO)_2(syn\text{-}\eta^3\text{-}C_5H_7)PR_3$ (PR_3 = PMe_3 (**6a**), $P(OH_3)_3$ (**6b**)). Complex **5a** does not react with CO, CH_3CN, and acetone to achieve an 18-electron configuration. An X-ray diffraction study of **6a** has been performed. The ORTEP drawing is shown in Figure 5, and the selected bond distances and angles are given in Table III. The coordination geometry about the molybdenum atom is approximately an octahedron with the atoms N1, N3, P, C24, and C25 and an allyl group occupying the six coordination sites. The N1 and N3 atoms are trans to the two carbonyls, and the phosphorus atom is cis to the pentadienyl group. The Mo···B distance is 3.759 (11) Å, significantly longer than that of **5a** (3.226 (12) Å). The chelate pyrazole ring is buckled into a boat conformation with the two pyrazole groups tilting toward the phosphate atom and the boron atom bending toward the pentadienyl group. Notably, the two phenyl groups bend outward from the molybdenum atom, and this conformation is distinct from that of **5a**.

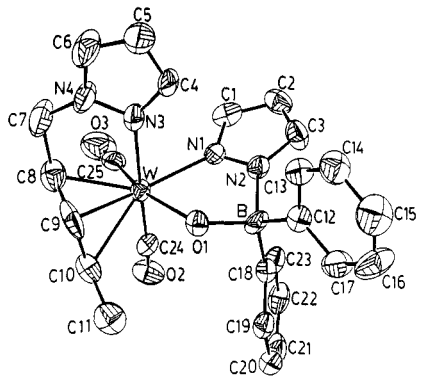

Figure 6. ORTEP drawing of **7b**.

The Mo-N1 (2.251 (8) Å) and Mo-N3 (2.250 (8) Å) distances are nearly equal but, however, are longer than those of **5** (2.143 (9), 2.172 (9) Å). Apparently, the increasing electron density on the molybdenum center contributed by PMe_3 tends to increase the Mo-N bond distances. The pentadienyl group has a staggered orientation with respect to the P-C24-C25 face. The C-C bond lengths in the pentadienyl moiety represent a pattern common to those of other *syn*-η^3-pentadienyl complexes.

Stirring of a wet tetrahydrofuran solution of **5a** produced the yellow solid **7a** depicted below. The yield was 20% for a reaction time of 5–6 h. A prolonged reaction time

$(C_6H_5)_2B(pz)_2M(CO)_2(\eta^3\text{-}C_5H_7)$ $\xrightarrow[23\ °C,\ 5\text{–}6\ h]{H_2O/THF}$

M = Mo (**5a**), W (**5b**)

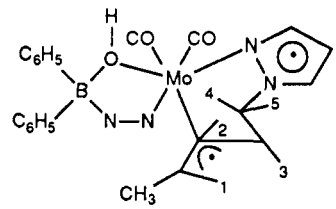

M = Mo (**7a**), W (**7b**)

led to a drastic decrease in yield. In view of such a complicated structure, crystallographic study is essential for structural characterization even though the elemental analysis and NMR and IR spectra are compatible with the given formula. Because an X-ray diffraction study of **7a** was hampered by its poor crystallinity, however, we turned to the synthesis of the tungsten analogue (**7b**). Interestingly, the reaction between $W(CO)_2(CH_3CN)_2(\eta^3\text{-}C_5H_7)Br$[11b] and $Na(C_6H_5)_2Br(pz)_2$ gave **7b** and $(C_6H_5)_2B(pz)_2W(CO)_2(\eta^3\text{-}C_5H_7)$ (**5b**). Complex **7b** presumably arises from the hydrolysis of **5b**. Attempts to isolate **5b** in pure form by column chromatography were hampered by its facile transformation to **7b** during column elution. Indeed, for an NMR sample of the crude product containing both **5b** and **7b** to which was added a minor portion of D_2O in acetone-d_6, the proton signals of **7b** gradually increased whereas the signals of **5b** slowly disappeared.

The molecular structure of **7b** has been determined, and its ORTEP drawing is given in Figure 6. It is clear that H_2O has cleaved the B-N bond and the N-N bond of the cleaved pyrazole group undergoes 1,5-addition to the η^3-pentadienyl group to form a η^3-1-pyrazolyl-3-penten-2-yl ligand. The coordination geometry around the tungsten atom is approximately an octahedron with the atoms N1, N3, O1, C25, and C24 and an allyl group occupying the six coordination sites. The W-N3 distance (2.240 (8) Å) is longer than that of W-N1 (2.176 (8) Å). The η^3-pentenyl configuration is W-shaped, and the allyl mouth faces the N1-C24-C25 direction. The C8-C9 (1.432 (20) Å) and

Table IV. Selected Bond Distances (Å) and Bond Angles (deg) for 7b

W-N1	2.176 (8)	C7-C8	1.518 (17)
W-N3	2.240 (8)	C8-C9	1.432 (20)
W-C8	2.273 (11)	C9-C10	1.425 (16)
W-C9	2.195 (9)	C10-C11	1.473 (17)
W-C10	2.382 (10)	C12-B	1.579 (16)
W-C24	1.944 (10)	C18-B	1.624 (15)
W-C25	1.868 (10)	C24-O2	1.175 (12)
W-O1	2.194 (6)	C25-O3	1.201 (13)
N2-B	1.577 (13)	O1-B	1.521 (12)
N4-C7	1.419 (15)		
N1-W-N3	79.9 (3)	C24-W-O1	97.4 (4)
N1-W-C8	145.0 (4)	C25-W-O1	163.5 (3)
N1-W-C9	156.0 (3)	W-N1-N2	120.1 (6)
N1-W-C10	151.4 (4)	N1-N2-B	117.2 (8)
N1-W-C24	96.8 (4)	W-N3-N4	118.2 (6)
N1-W-C25	92.2 (4)	N3-N4-C7	118.5 (8)
N1-W-O1	72.4 (3)	N4-C7-C8	109.8 (9)
N3-W-C8	72.5 (3)	W-C8-C7	113.0 (7)
N3-W-C9	81.7 (3)	W-C8-C9	68.4 (6)
N3-W-C10	116.5 (3)	C7-C8-C9	122.3 (10)
N3-W-C24	174.6 (4)	W-C9-C8	74.3 (6)
N3-W-C25	97.6 (4)	W-C9-C10	79.2 (6)
N3-W-O1	85.5 (3)	C8-C9-C10	117.2 (10)
C8-W-C9	37.3 (5)	W-C10-C9	64.8 (5)
C8-W-C10	63.1 (4)	W-C10-C11	121.7 (7)
C8-W-C24	109.0 (4)	C9-C10-C11	126.8 (10)
C8-W-C25	71.1 (4)	W-C24-O2	173.4 (11)
C8-W-O1	125.0 (3)	W-C25-O3	175.3 (9)
C9-W-C10	36.0 (4)	W-O1-B	119.3 (5)
C9-W-C24	102.7 (4)	N2-B-C12	108.8 (9)
C9-W-C25	105.4 (5)	N2-B-C18	109.0 (8)
C9-W-O1	91.1 (4)	N2-B-O1	99.9 (7)
C10-W-C24	68.3 (4)	C12-B-C18	117.7 (8)
C10-W-C25	107.5 (4)	C12-B-O1	112.2 (8)
C10-W-O1	85.1 (3)	C18-B-O1	107.8 (8)
C24-W-C25	78.3 (5)		

C9–C10 (1.425 (16) Å) bonds are longer than those of C7–C8 (1.518 (17) Å) and C10–C11 (1.473 (17) Å). The W–O1 bond length (2.194 (6) Å) is rational in comparison with the known W^{II}–O bond lengths.[27]

In a deuterium-labeling experiment, integration of the ^1H NMR spectrum of **7a** resulting from the reaction between D_2O and **5a** revealed that D^+ adds at the allyl methyl group. On the basis of this result, we propose a plausible mechanism depicted in Scheme III. The H_2O molecule first coordinates to the metal center to form the 18e species III. In III, the bound H_2O molecule cleaves the B–N bond, yielding species IV. Further coupling of the allyl group and pyrazole group produces the ion V, which further undergoes transformation to yield the product. During the protonation process the CH_2^- terminus of V can be protonated by H_2O or acidic ^+N–H as both mechanisms are compatible with the labeling experiment.

Conclusions

The reactions between $AgXF_n$ (XF_n = BF_4, PF_6) and $Mo(N\frown N)(CO)_2(\eta^3\text{-}C_5H_7)Br$ (N⌒N = bpy, phen) in CH_2Cl_2 yield $(\eta^3\text{-}C_5H_7)Mo(N\frown N)(CO)_2XF_n$. Spectroscopic data show that, herein, PF_6 and BF_4^- serve as η^1-coordinating ligands. In donor solvents (S), the molybdenum(II) ion loses the BF_4^- anion to form $[(\eta^3\text{-}C_5H_7)Mo(N\frown N)(CO)_2S]BF_4$, which exists as several stereoisomers. The chemical-exchanging phenomenon of these stereoisomers has been established by a ^1H spin-saturation experiment. An X-ray structure of one stereoisomer of $[(\eta^3\text{-}C_5H_7)Mo(bpy)(CO)_2(CH_3CN)]PF_6$ has been presented. The reaction between $(\eta^3\text{-}C_5H_7)Mo(CO)_2(CH_3CN)_2Br$ and $Na(C_6H_5)_2B(pz)_2$ yields the 16-electron compound $(\eta^3\text{-}C_5H_7)Mo(CO)_2[(C_6H_5)_2B(pz)_2]$, for which the solid-state structure has been deduced. In solution, the complex exhibits a stereochemically nonrigid structure, and the dynamic process has been characterized by variable-temperature NMR spectra. The reaction of H_2O and **5a** gives $[(C_6H_5)_2B(pz)(OH)Mo(\eta^3\text{-}NNCHCHCHCH_2CHCHCHCH_3)(CO)_2]$ (**7a**) in moderate yield. The crystal structure of **7a** was determined from that of its tungsten analogue (**7b**).

Scheme III

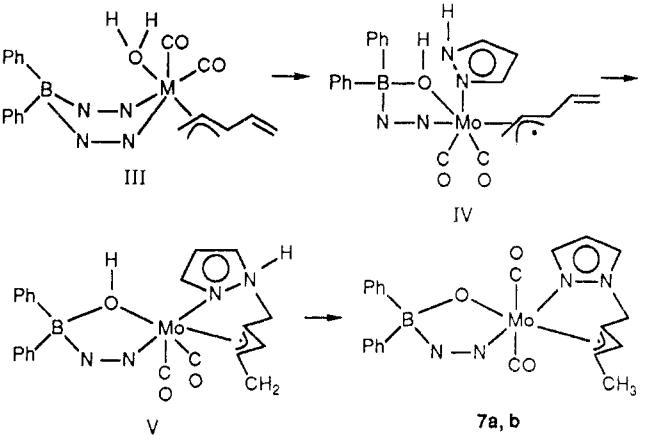

Experimental Section

(a) General Procedures and Measurements. All operations were performed under a nitrogen atmosphere and with use of standard Schlenk tube techniques. The ^1H (400 MHz), ^{13}C (100 MHz), ^{19}F (93.6 MHz), and ^{31}P (48.25 MHz) NMR experiments were performed on either a Bruker AM 400 or a JEOL-100 spectrometer. The chemical shifts in ^1H and ^{13}C, ^{19}F, and ^{31}P NMR spectra were referenced to tetramethylsilane, $CFCl_3$, and H_3PO_4, respectively. Infrared spectra were recorded on a Perkin-Elmer 781 spectrometer. Elemental analyses were performed by the Microanalytic Laboratory, Department of Chemistry, National Taiwan University, Taipei, Taiwan. $Mo(CO)_6$, bipyridine, phenanthroline, $AgBF_4$, and $AgPF_6$ were obtained from Strem Chemicals and used without further purification; 1-Bromopenta-2,4-diene[28] and $(\eta^3\text{-}C_5H_7)Mo(CO)_2(CH_3CN)_2Br$[8] were prepared according to the literature.

(b) Synthesis of $Mo(bpy)(CO)_2(\eta^3\text{-}C_5H_7)Br$ (1a). 2,2′-Bipyridine (0.82 g, 5.01 mmol) was slowly added to a 20-mL dichloromethane solution of $Mo(CO)_2(\eta^3\text{-}C_5H_7)(CH_3CN)_2Br$ (1.91 g, 5.00 mmol), and the mixture was stirred at 23 °C for 20 min. After removal of the solvent under reduced pressure, the residues were recrystallized from CH_2Cl_2–hexane to yield a dark red powder of **1a** (2.24 g, 4.80 mmol). IR (Nujol): ν(CO) 1940 (s) and 1850 (s) cm^{-1}; ν(C=C) 1600 (s) cm^{-1}. ^1H NMR (400 MHz, DMF-d_7): δ 0.57 (dd, 1 H, H^1), 1.73 (t, 1 H, H^4), 2.34 (dd, 1 H, H^2), 2.94 (td, 1 H, H^3), 4.36 (dd, 1 H, H^7), 4.67 (dd, 1 H, H^6), 4.79 (dt, 1 H, H^5), 6.88, 7.43, 7.89 (t, d, d, 8 H), J_{12} = 1.7 Hz, J_{13} = 9.4 Hz, J_{23} = 6.4 Hz, J_{34} = 10.0 Hz, J_{45} = 10.2 Hz, J_{57} = 10.1 Hz, J_{56} = 17.0 Hz. ^{13}C NMR (100 MHz, DMF-d_7, selected peaks): δ 54.0 (CH^1H^2), 74.7, 85.5 (CH^3 + CH^4), 118.3 (CH^6H^7), 138.2 (CH^5), 224.6, 227.3 (2 CO). Anal. Calcd for $MoC_{17}H_{15}O_2N_2Br$: C, 42.61; H, 3.32; N, 6.15. Found: C, 42.58; H, 3.31; N, 6.13.

(c) Synthesis of $Mo(phen)(CO)_2(\eta^3\text{-}C_5H_7)Br$ (1b). This complex was prepared similarly from the reaction between phenanthroline and $Mo(CO)_2(\eta^3\text{-}C_5H_7)(CH_3CN)_2Br$ in CH_2Cl_2; the yield is 86%. IR spectrum (Nujol): ν(C=C) 1620 (w) cm^{-1}; ν(CO) 1944 (s) and 1850 (s) cm^{-1}. ^1H NMR (400 MHz, DMF-d_7): δ 1.43 (dd, 1 H, H^1), 2.49 (t, 1 H, H^4), 3.10 (dd, 1 H, H^2), 3.17 (m,

(27) (a) Fischer, E. O.; Friedrich, P. *Angew. Chem.* **1979**, *91*, 345. (b) Bokii, N. G.; Gatilor, Y. V.; Struchkov, Y. T.; Ustynyuk, N. A. *J. Organomet. Chem.* **1973**, *54*, 213.

(28) Miginiac, P. *Justus Liebigs Ann. Chem.* **1962**, 445.

1 H, H^3), 5.01 (m, 1 H, H^5), 5.12 (d, 1 H, H^7), 5.42 (d, 1 H, H^6), 7.72, 7.78, 8.24, 8.40, 8.71, 8.78, 9.09 (d, d, d, d, d, d, t, t, 8 H, phen H^1), J_{12} = 2.0 Hz, J_{13} = 9.5 Hz, J_{23} = 6.2 Hz, J_{34} = 9.7 Hz, J_{45} = 10.0 Hz, J_{57} = 10.2 Hz, J_{56} = 16.8 Hz. Anal. Calcd for $MoC_{19}H_{15}O_2N_2Br$: C, 50.13; H, 3.15; N, 5.56. Found: C, 49.93; H, 3.09; N, 5.39.

(d) Synthesis of Mo(bpy)(CO)$_2$(η^3-C$_5$H$_7$)(η^1-BF$_4$) (2a). $AgBF_4$ (0.12 g, 0.60 mmol) was added to complex **1a** (0.27 g, 0.58 mmol) in 20 mL of CH_2Cl_2 with rapid stirring at 0 °C for 1 h. After removal of insoluble AgBr by filtration, the solution was evaporated to dryness to afford a dark red powder. Recrystallization from a saturated CH_2Cl_2–hexane solution yielded a dark red crystalline solid. IR (CH_2Cl_2): ν(C=C) 1628 (w) cm^{-1}; ν(CO) 1945 (s) and 1859 (s) cm^{-1}. ^{1}H NMR (400 MHz, CD_2Cl_2): δ 1.68 (d, 1 H, H^1), 2.52 (t, 1 H, H^4), 3.20 (d, 1 H, H^2), 3.45 (m, 1 H, H^3), 5.10 (d, 1 H, H^7), 5.40 (d, 1 H, H^6), 5.52 (m, 1 H, H^5), 7.2–9.0 (8 H, bpy), J_{13} = 10.4 Hz, J_{23} = 6.2 Hz, J_{34} = 10.0 Hz, J_{45} = 10.2 Hz, J_{56} = 17.2 Hz, J_{67} = 10.3 Hz. ^{13}C NMR (100 MHz, CD_2Cl_2) selected peaks): δ 56.2 (CH^1H^2), 79.3, 82.4 (CH^3 + CH^4), 117.8 (CH^6H^7), 140.4 (CH^5). ^{19}F NMR (93.6 MHz, CH_2Cl_2 –60 °C): δ –148.2 (d, 3 F, $J_{FF'}$ = 88 Hz), –144.2 (q, 1 F, $J_{FF'}$ = 88 Hz). Anal. Calcd for $MoC_{17}H_{15}O_2N_2BF_4$: C, 43.75; H, 3.67; N, 5.15. Found: C, 43.82; H, 3.82; N, 5.38.

(e) Synthesis of Mo(phen)(CO)$_2$(η^3-C$_5$H$_7$)(η^1-BF$_4$) (2b). $AgBF_4$ (0.12 g, 0.60 mmol) was added to complex **1b** (0.27 g, 0.60 mmol) in 20 mL of CH_2Cl_2, and the solution was stirred rapidly at 0 °C for 1 h. After removal of insoluble AgBr by filtration, the solution was evaporated to dryness to afford a dark red powder. Recrystallization from a saturated CH_2Cl_2–hexane solution yielded a dark red crystalline solid. IR (CH_2Cl_2): ν(C=C) 1630 (w) cm^{-1}; ν(CO) 1945 (s) and 1850 (s) cm^{-1}. ^{1}H NMR (400 MHz, CD_2Cl_2): δ 1.70 (d, 1 H, H^1), 2.50 (t, 1 H, H^4), 3.00 (d, 1 H, H^2), 3.30 (m, 1 H, H^3), 5.18 (d, 1 H, H^7), 5.40 (d, 1 H, H^6), 5.50 (m, 1 H, H^5), 7.2–9.0 (8 H, phen), J_{13} = 10.2 Hz, J_{23} = 6.2 Hz, J_{34} = 10.0 Hz, J_{45} = 10.1 Hz, J_{56} = 17.1 Hz, J_{67} = 10.2 Hz. ^{13}C NMR (100 MHz, CD_2Cl_2), selected peaks): δ 55.8 (CH^1H^2), 79.2, 81.5 (CH^3 + CH^4), 119.5 (CH^6H^7), 140.2 (CH^5). ^{19}F NMR (93.6 MHz, CH_2Cl_2, –40 °C): δ –146.4 (d, 3 F, $J_{FF'}$ = 99 Hz), –142.3 (q, 1 F, $J_{FF'}$ = 99 Hz). Anal. Calcd for $MoC_{19}H_{15}O_2N_2BF_4$: C, 46.95; H, 3.11; N, 5.76. Found: C, 46.91; H, 3.08; N, 5.76.

(f) Synthesis of [Mo(bpy)(CO)$_2$(η^3-C$_5$H$_7$)(CH$_3$CN)]BF$_4$ (3a). Silver tetrafluoroborate (0.12 g, 0.59 mmol) was added to **1a** (0.27 g, 0.58 mmol) in a rapidly stirred CH_3CN solution at 0 °C for 30 min. The solution was filtered to remove silver bromide and evaporated to dryness. The residues were recrystallized from a saturated CH_2Cl_2–ether solution to afford red-orange block-shaped crystals of **3a** (0.32 g, 0.56 mmol). IR (Nujol): ν(C=C) 1630 (w) cm^{-1}; ν(CO) 1940 (s) and 1860 (w) cm^{-1}. ^{1}H NMR (400 MHz, CD_3CN): major isomer, δ 1.51 (s, 3 H, CH_3CN), 1.78 (dd, 1 H, H^1), 2.95 (1 H, t, H^4), 3.63 (dd, 1 H, H^2), 4.61 (td, 1 H, H^3), 5.37 (dd, 1 H, H^6), 5.67 (dd, 1 H, H^7), 6.22 (m, 1 H, H^5), 8.0–10.1 (8 H, bpy′ H), J_{13} = 9.0 Hz, J_{12} = 2.6 Hz, J_{23} = 6.7 Hz, J_{34} = 9.0 Hz, J_{45} = 9.2 Hz, J_{56} = 16.7 Hz, J_{57} = 10.2 Hz; minor isomer, δ 1.51 (s, 3 H, CH_3CN), 1.80 (d, 1 H, H^1), 3.02 (t, 1 H, H^4), 3.53 (m, 1 H, H^4), 3.65 (d, 1 H, H^2), 5.37 (d, 1 H, H^7), 5.65 (m, 1 H, H^5), 5.67 (d, 1 H, H^6), 8.0–10.1 (8 H, bpy′ H), J_{13} = 9.1 Hz, J_{23} = 6.6 Hz, J_{34} = 9.2 Hz, J_{45} = 10.2 Hz, J_{56} = 16.9 Hz, J_{57} = 10.3 Hz. ^{13}C NMR (100 MHz, CD_3CN, selected peaks): major isomer, δ 53.6 (CH^1H^2), 74.5, 85.4 (CH^3 + CH^4), 119.4 (CH^6H^7), 138.4 (CH^5); minor isomer, δ 55.2 (CH^1H^2), 78.2, 84.4 (CH^3 + CH^4), 110.4 (CH^6H^7), 140.8 (CH^3). Anal. Calcd for $MoC_{19}H_{18}O_2N_2BF_4$: C, 38.61; H, 3.06; N, 7.11. Found: C, 38.45; H, 2.97; N, 7.02.

(g) Synthesis of [Mo(phen)(CO)$_2$(η^3-C$_5$H$_7$)(CH$_3$CN)]BF$_4$ (4a). Silver tetrafluoroborate (0.12 g, 0.59 mmol) was added to **1b** (0.35 g, 0.60 mmol) in a rapidly stirred CH_3CN solution at 0 °C for 30 min. The solution was filtered to remove silver bromide and evaporated to dryness. The residues were recrystallized from a CH_2Cl_2–ether solution to afford red-orange blocks of **4a** (0.23 g, 0.43 mmol). IR (Nujol): ν(C=C) 1630 (w) cm^{-1}; ν(CO) 1940 (s) and 1860 (s) cm^{-1}. ^{1}H NMR (400 MHz, CD_3CN): major isomer, δ 1.51 (s, 3 H, CH_3CN), 1.78 (dd, 1 H, H^1), 2.95 (t, 1 H, H^4), 3.63 (dd, 1 H, H^2), 4.61 (m, 1 H, H^3), 5.37 (d, 1 H, H^7), 5.67 (d, 1 H, H^6), 6.22 (m, 1 H, H^5), 8.0–10.1 (8 H, phen′ H); minor isomer, δ 1.51 (s, 3 H, CH_3CN), 1.79 (d, 1 H, H^1), 3.02 (t, 1 H, H^4), 3.53 (m, 1 H, H^3), 3.65 (d, 1 H, H^2), 5.36 (d, 1 H, H^7), 5.65 (m, 1 H, H^5), 5.67 (d, 1 H, H^6), 8.0–10.1 (8 H, phen′ H), J_{13} = 10.11 Hz, J_{23} = 6.6 Hz, J_{34} = 9.1 Hz, J_{43} = 10.1 Hz, J_{56} = 18.1 Hz, J_{67} = 10.3 Hz. ^{13}C NMR (100 MHz, CD_3CN, selected peaks): major isomer, δ 53.6 (CH^1H^2), 74.5, 85.4 (CH^3 + CH^4), 119.3 (CH^6H^7), 156.4 (CH^5); minor isomer, δ 55.2 (CH^1H^2), 78.2, 84.3 (CH^3 + CH^4), 118.8 (CH^6H^7), 148.8 (CH^5). Anal. Calcd for $MoC_{21}H_{18}O_2N_3BF_4$: C, 45.76; H, 3.29; N, 7.62. Found: C, 45.64; H, 3.19; N, 7.58.

(h) Synthesis of [Mo(bpy)(CO)$_2$(η^3-C$_5$H$_7$)(CH$_3$COCH$_3$)]BF$_4$ (3b). Silver tetrafluoroborate (0.12 g, 0.58 mmol) was added to **1a** (0.29 g, 0.59 mmol) in 20 mL of rapidly stirred CH_3COCH_3 solution at 0 °C for 30 min. The solution was filtered and evaporated to dryness. The residues were recrystallized from CH_2Cl_2–ether to afford orange block-shaped crystals (0.18 g, 0.36 mmol). IR (Nujol): ν(C=C) 1635 (w) cm^{-1}; ν(CO) 1948 (s), 1857 (s), 1688 (s) cm^{-1}. ^{1}H NMR (400 MHz, CD_3COCD_3): isomer a, δ 1.49 (dd, 1 H, H^1), 2.30 (s, 6 H, $(CH_3)_2CO$), 2.98 (t, 1 H, H^4), 3.53 (dd, 1 H, H^2), 4.45 (m, 1 H, H^3), 5.19 (d, 1 H, H^7), 5.38 (d, 1 H, H^6), 6.62 (m, 1 H, H^5), 8.1–10.3 (8 H, bpy′ H), J_{12} = 2.9 Hz, J_{13} = 10.0 Hz, J_{23} = 6.4 Hz, J_{34} = 10.0 Hz, J_{45} = 9.8 Hz, J_{56} = 17.2 Hz, J_{57} = 10.3 Hz; isomer b, δ 1.68 (d, 1 H, H^1), 2.58 (s, 6 H, $(CH_3)_2CO$), 3.08 (t, 1 H, H^4), 3.35 (d, 1 H, H^2), 3.59 (m, 1 H, H^3), 5.19 (d, 1 H, H^7), 5.30 (d, 1 H, H^6), 5.50 (m, 1 H, H^5), 7.85–10.10 (8 H, bpy), J_{13} = 9.8 Hz, J_{23} = 6.2 Hz, J_{34} = 9.8 Hz, J_{45} = 9.8 Hz, J_{56} = 17.0 Hz, J_{57} = 10.4 Hz; isomer c, δ 1.50 (d, 1 H, H^1), 3.08 (t, 1 H, H^4), 3.85 (d, 1 H, H^2), 4.45 (m, 1 H, H^1), 5.30 (d, 1 H, H^6), 5.55 (d, 1 H, H^7), 6.50 (m, 1 H, H^5), 7.5–10.0 (8 H, bpy′ H), J_{13} = 10.2 Hz, J_{23} = 6.6 Hz, J_{34} = 10.0 Hz, J_{45} = 10.3 Hz, J_{56} = 17.8 Hz, J_{67} = 10.4 Hz; isomer d, δ 1.38 (d, 1 H, H^1), 2.50 (t, 1 H, H^4), 3.60 (m, 1 H, H^3), 3.85 (d, 1 H, H^2), 5.30 (d, 1 H, H^6), 5.60 (d, 1 H, H^7), 6.15 (m, 1 H, H^5), 7.5–10.0 (8 H, bpy′ H), J_{13} = 10.0 Hz, J_{23} = 6.0 Hz, J_{34} = 9.8 Hz, J_{45} = 9.6 Hz, J_{56} = 17.2 Hz, J_{57} = 10.4 Hz. Anal. Calcd for $MoC_{20}H_{21}O_3N_2BF_4$: C, 46.18; H, 4.07; N, 5.39. Found: C, 45.93; H, 3.98; N, 5.22.

(i) Synthesis of [Mo(phen)(CO)$_2$(η^3-C$_5$H$_7$)(CH$_3$COCH$_3$)]BF$_6$ (4b). This complex was prepared similarly from the reaction between $AgBF_4$ and **1b** in an acetone solution; the yield was 45%. IR (Nujol): ν(C=C) 1633 (w) cm^{-1}; ν(CO) 1947 (s), 1856 (s), 1680 (s), cm^{-1}. ^{1}H NMR (400 MHz, CD_3COCD_3): isomer a, δ 1.59 (d, 1 H, H^1), 3.01 (t, 1 H, H^4), 3.78 (d, 1 H, H^2), 4.65 (m, 1 H, H^3), 5.23 (d, 1 H, H^7), 5.60 (d, 1 H, H^6), 6.54 (m, 1 H, H^5), 8.0–10.0 (8 H, phen′ H), J_{13} = 10.2 Hz, J_{23} = 6.2 Hz, J_{24} = 10.1 Hz, J_{45} = 9.8 Hz, J_{56} = 17.8 Hz, J_{57} = 10.0 Hz; isomer b, δ 1.53 (d, 1 H, H^1), 3.20 (t, 1 H, H^4), 4.02 (d, 1 H, H^2), 4.80 (m, 1 H, H^3), 5.26 (d, 1 H, H^7), 5.73 (d, 1 H, H^6), 5.50 (m, 1 H, H^5), 8.0–10.0 (8 H, phen′ H), J_{13} = 10.1 Hz, J_{23} = 6.4 Hz, J_{34} = 10.1 Hz, J_{45} = 9.6 Hz, J_{56} = 17.4 Hz, J_{57} = 10.0 Hz; isomer c, δ 1.48 (d, 1 H, H^1), 3.14 (t, 1 H, H^4), 3.85 (d, 1 H, H^2), 4.40 (m, 1 H, H^3), 5.34 (d, 1 H, H^6), 5.49 (d, 1 H, H^7), 6.50 (m, 1 H, H^5), 7.5–10.0 (8 H, phen′ H), J_{13} = 10.3 Hz, J_{23} = 6.4 Hz, J_{34} = 10.0 Hz, J_{45} = 10.1 Hz, J_{56} = 17.4 Hz, J_{67} = 10.5 Hz; isomer d, δ 1.32 (d, 1 H, H^1), 2.43 (t, 1 H, H^4), 3.55 (m, 1 H, H^3), 3.85 (d, 1 H, H^2), 5.34 (d, 1 H, H^6), 5.62 (d, 1 H, H^7), 6.10 (m, 1 H, H^5), 7.5–10.0 (8 H, phen′ H), J_{13} = 10.1 Hz, J_{23} = 6.4 Hz, J_{34} = 9.6 Hz, J_{45} = 9.2 Hz, J_{56} = 17.4 Hz, J_{67} = 10.2 Hz. Anal. Calcd for $MoC_{22}H_{21}O_3N_2BF_4$: C, 48.51; H, 3.67; N, 5.15. Found: C, 48.74; H, 3.82; N, 5.20.

(j) Synthesis of [Mo(CO)$_2$(bpy)(η^3-C$_5$H$_7$)(ether)]BF$_4$ (3c). Complex **2a** (0.28 g, 0.60 mmol) was dissolved in 20 mL of CH_2Cl_2, followed by addition of 10 mL of ether. The mixture was stirred for 2 h at 0 °C and evaporated to dryness. The residues were recrystallized from a saturated CH_2Cl_2–hexane solution to afford a dark orange powder (0.15 g, 0.28 mmol). IR (Nujol): ν(C=C) 1638 (w) cm^{-1}; ν(CO) 1948 (s), 1868 (s) cm^{-1}. ^{1}H NMR (400 MHz, CD_2Cl_2): isomer a, δ 1.74 (dd, 1 H, H^1), 2.89 (t, 1 H, H^4), 3.40 (dd, 1 H, H^2), 3.72 (m, 1 H, H^3), 5.21 (d, 1 H, H^7), 5.58 (d, 1 H, H^6), 6.49 (m, 1 H, H^5), 8.0–10.0 (8 H, bpy), J_{13} = 10.3 Hz, J_{23} = 6.4 Hz, J_{34} = 10.2 Hz, J_{45} = 9.8 Hz, J_{56} = 17.2 Hz, J_{57} = 10.0 Hz; isomer b, δ 1.88 (d, 1 H, H^1), 2.89 (m, 1 H, H^3), 3.06 (t, 1 H, H^4), 3.23 (d, 1 H, H^2), 5.21 (d, 1 H, H^7), 5.49 (m, 1 H, H^5), 5.58 (d, 1 H, H^6), 8.0–10.0 (8 H, bpy), J_{13} = 10.2 Hz, J_{23} = 6.3 Hz, J_{34} = 10.1 Hz, J_{45} = 9.6 Hz, J_{56} = 17.3 Hz, J_{57} = 10.2 Hz; isomer c, δ 1.52 (d, 1 H, H^1), 3.22 (t, 1 H, H^4), 3.78 (d, 1 H, H^2), 4.52 (m, 1 H, H^3), 5.40 (d, 1 H, H^6), 5.52 (d, 1 H, H^7), 6.55 (m, 1 H, H^5), 7.5–10.0 (8 H, bpy), J_{13} = 10.3 Hz, J_{23} = 6.4 Hz, J_{34} = 10.0 Hz, J_{45} = 10.1 Hz, J_{56} = 17.2 Hz, J_{67} = 10.5 Hz; isomer d, δ 1.49 (d, 1 H, H^1), 2.38 (t, 1 H, H^4), 3.60 (m, 1 H, H^3), 3.90 (d, 1 H, H^2), 5.34 (d, 1 H, H^6), 5.58 (d, 1 H, H^7), 6.04 (m, 1 H, H^5), 7.5–9.8 (8 H, bpy), J_{13} = 10.1 Hz, J_{23} = 6.5 Hz, J_{34} = 9.6 Hz, J_{45} = 9.2 Hz, J_{56} = 17.2 Hz, J_{57}

Table V. Summary of Crystal Data and Intensity Collection

	3a	5a	6a	7b
formula	$C_{19}H_{18}N_3O_2F_6PMo$	$C_{25}H_{23}N_4O_2BMo$	$C_{28}H_{32}N_4O_2BPMo$	$C_{25}H_{25}N_4O_3BW$
cryst color	colorless	brick red	deep red	yellow
cryst size, mm	1.0 × 1.0 × 1.0	0.17 × 0.2 × 0.5	0.1 × 0.25 × 0.3	0.25 × 0.45 × 0.45
space group	$P\bar{1}$	$P\bar{1}$	$P2_1/c$	$P2_12_12_1$
a, Å	8.107 (4)	9.951 (13)	14.552 (5)	10.0979 (21)
b, Å	11.055 (3)	10.435 (7)	9.711 (2)	13.6753 (23)
c, Å	13.118 (3)	12.210 (8)	19.862 (8)	17.331 (3)
α, deg	106.42 (2)	82.31 (6)	90	90
β, deg	95.39 (3)	79.27 (9)	90.48 (3)	90
γ, deg	96.41 (3)	74.62 (10)	90	90
Z	2	2	4	4
calcd density, Mg/m^3	1.678	1.439	1.407	1.741
abs coeff, cm^{-1}	7.15	5.6	5.4	49.6
F(000)	560	528	1220	1180
diffractometer	Nicolet R3m/V	Nonius CAD4	Nonius CAD4	Nonius CAD4
radiation	Mo Kα	Mo Kα	Mo Kα	Mo Kα
2θ range, deg	2.5–49.0	2–50	2–50	2–54.8
scan param	1.2 plus Kα separation	1.0 + 0.35 tan θ	0.70 + 0.35 tan θ	0.80 + 0.35 tan θ
scan type	$\theta/2\theta$	$\theta/2\theta$	$\theta/2\theta$	$\theta/2\theta$
no. of indep rflns	3722, 2624 (>3$\sigma(I)$)	3117, 2368 (>2$\sigma(I)$)	3664, 1421 (>2$\sigma(I)$)	3087, 2650 (>2$\sigma(I)$)
weight scheme (w^{-1})	$\sigma^2(F) + 0.0012F^2$	$\sigma^2(F)$	$\sigma^2(F)$	$\sigma^2(F)$
final R, R_w, %	3.98, 4.10	6.7, 7.4	4.2, 3.6	3.2, 2.7
goodness of fit	0.98	4.72	1.32	1.82
largest Δ/σ	0.25	0.24	0.34	0.01
data to param ratio	7.7:1	7.9:1	4.3:1	8.6:1
largest diff peak, e/Å^3	0.49	1.14	0.39	0.92
largest diff hole, e/Å^3	−0.36	−1.07	−0.35	−1.08

= 10.2 Hz. Anal. Calcd for $C_{21}H_{25}N_2O_3MoBF_4$: C, 47.01; H, 4.66; N, 5.22. Found: C, 47.24; H, 4.72; N, 5.34.

(k) Synthesis of [Mo(CO)$_2$(phen)(η^3-C$_5$H$_7$)(ether)]BF$_4$ (4c). This complex was similarly prepared from the reaction between **2b** and ether in CH_2Cl_2 solution; the yield is 48% after recrystallization from a saturated CH_2Cl_2–hexane solution. IR (Nujol): ν(C=C) 1635 (w) cm^{-1}; ν(CO) 1948 (s), 1865 (s) cm^{-1}. ^{1}H NMR (400 MHz, CD_2Cl_2): isomer a, δ 1.76 (dd, 1 H, H^1), 2.89 (t, 1 H, H^4), 3.40 (dd, 1 H, H^2), 3.68 (m, 1 H, H^3), 5.24 (d, 1 H, H^7), 5.58 (d, 1 H, H^6), 6.49 (m, 1 H, H^5), 8.0–10.0 (8 H, bpy), J_{13} = 10.3 Hz, J_{23} = 6.5 Hz, J_{34} = 10.3 Hz, J_{45} = 9.7 Hz, J_{56} = 17.5 Hz, J_{57} = 10.2 Hz; isomer b, δ 1.80 (d, 1 H, H^1), 2.70 (m, 1 H, H^3), 2.96 (d, 1 H, H^4), 3.19 (d, 1 H, H^2), 5.21 (d, 1 H, H^7), 5.50 (m, 1 H, H^5), 5.62 (1 H, d, H^6), 8.0–10.0 (8 H, bpy), J_{13} = 10.3 Hz, J_{23} = 6.0 Hz, J_{34} = 10.2 Hz, J_{45} = 9.5 Hz, J_{56} = 17.0 Hz, J_{57} = 10.1 Hz; isomer c, δ 1.52 (d, 1 H, H^1), 3.20 (t, 1 H, H^4), 3.78 (d, 1 H, H^2), 4.52 (m, 1 H, H^2), 5.40 (d, 1 H, H^6), 5.48 (d, 1 H, H^7), 6.49 (m, 1 H, H^5), 7.5–10.0 (8 H, bpy), J_{13} = 10.4 Hz, J_{23} = 6.0 Hz, J_{34} = 10.0 Hz, J_{45} = 10.1 Hz, J_{56} = 17.2 Hz, J_{67} = 10.2 Hz; isomer d, δ 1.45 (d, 1 H, H^1), 2.35 (t, 1 H, H^4), 3.52 (m, 1 H, H^3), 3.92 (d, 1 H, H^2), 5.34 (d, 1 H, H^6), 5.54 (d, 1 H, H^7), 6.04 (m, 1 H, H^5), 7.5–9.8 (8 H, bpy), J_{13} = 10.2 Hz, J_{23} = 6.5 Hz, J_{34} = 9.2 Hz, J_{45} = 9.2 Hz, J_{56} = 17.1 Hz, J_{57} = 10.2 Hz. Anal. Calcd for $MoC_{23}H_{25}O_3N_2BF_4$: C, 49.31; H, 4.05; N, 5.00. Found: C, 49.22; H, 4.41; N, 48.3.

(l) Synthesis of [(C$_6$H$_5$)$_2$B(pz)$_2$Mo(CO)$_2$(η^3-C$_5$H$_7$)] (5a). Sodium diphenyldipyrazolylborate (0.16 g, 0.49 mmol) was added to Mo(CO)$_2$(CH$_3$CN)$_2$(η^3-C$_5$H$_7$)Br (0.19 g, 0.50 mmol) in 50 mL of CH_2Cl_2 and stirred at 23 °C for 30 min. The solvent was then removed in vacuo, and the residue was chromatographed through a neutral alumina column with dichloromethane as the eluting solvent. A yellow band was slowly developed and collected. Removal of the solvent under reduced pressure gave a yellow powder (0.10 g, 0.19 mmol); the yield is 38%. ^{1}H NMR (400 MHz, toluene-d_8, −40 °C): δ 0.57 (d, 1 H, H^2), 0.65 (d, 1 H, H^1), 2.91 (m, 1 H, H^3), 2.65 (t, 1 H, H^4), 5.29 (d, 1 H, H^7), 5.44 (d, 1 H, H^6), 6.02 (m, 1 H, H^5), 5.8–9.0 (16 H, (C$_6$H$_5$)$_2$B(pz)$_2$), J_{13} = 8.9 Hz, J_{23} = 5.6 Hz, J_{34} = 9.0 Hz, J_{45} = 9.6 Hz, J_{56} = 17.1 Hz, J_{57} = 10.1 Hz. ^{13}C NMR (100 MHz, toluene-d_8, −40 °C, selected peaks): δ 49.6 (CH^{1}H^2), 80.7, 89.5 (CH^3 + CH^4), 118.0 (CH^{6}H^7), 1389 (CH^5), 228.1, 231.0 (2 Mo–CO). IR (CH_2Cl_2): ν(C=C) 1630 (w) cm^{-1}; ν(CO) 1943 (s), 1860 (s) cm^{-1}. Anal. Calcd for $MoC_{25}H_{23}O_2N_4B$: C, 57.94; H, 4.47; N, 10.81. Found: C, 57.93; H, 4.24; N, 10.64.

(m) Synthesis of [(C$_6$H$_5$)$_2$B(pz)$_2$Mo(CO)$_2$(PMe$_3$)(η^3-C$_5$H$_7$)] (6a). Trimethylphosphine (0.30 g, 0.40 mmol) was added to **5a** (0.21 g, 0.40 mmol) in 20 mL of CH_2Cl_2. The solution was stirred at 23 °C for 20 min and evaporated to dryness. The residue was chromatographed through a neutral alumina column with dichloromethane as the eluting solvent. A yellow band was developed and collected. Removal of the solvent under reduced pressure gave a yellow powder, which was recrystallized from a saturated CH_2Cl_2–hexane solution to yield red block-shaped crystals of **6a** (0.10 g, 0.19 mmol). IR (CH_2Cl_2): ν(C=C) 1603 (w) cm^{-1}; ν(CO) 1928 (s), 1835 (s) cm^{-1}. ^{1}H NMR (400 MHz, $CDCl_3$): δ 0.88 (d, 9 H, PMe$_3$), 1.59 (d, 1 H, H^1), 2.57 (t, 1 H, H^4), 2.96 (m, 1 H, H^3), 2.97 (d, 1 H, H^2), 4.92–4.94 (m, 2 H, H^6 + H^7), 5.25 (m, 1 H, H^5), 6.82–8.47 (16 H, Ph, pz), J_{13} = 10.2 Hz, J_{23} = 6.2 Hz, J_{34} = 10.2 Hz, J_{45} = 10.2 Hz, J_{57} = 9.8 Hz, J_{56} = 16.8 Hz. ^{13}C NMR (100 MHz, $CDCl_3$, selected peaks): δ 58.93 (CH^{1}H^2), 76.2, 85.1 (CH^3 + CH^4), 116.8 (CH^{6}H^7), 138.4 (CH^5), 227.0 (d, Mo–CO, J_{PC} = 10 Hz), 226.1 (d, Mo–CO, J_{PC} = 11 Hz). Anal. Calcd for $MoC_{28}H_{32}O_2N_4BP$: C, 56.59; H, 5.43; N, 9.43. Found: C, 56.43; H, 5.36; N, 9.41.

(n) Synthesis of [(C$_6$H$_5$)$_2$B(pz)$_2$Mo(CO)$_2$(P(OCH$_3$)$_3$)(η^3-C$_5$H$_7$)] (6b). This complex is prepared similarly from the reaction between **5a** and P(OCH$_3$)$_3$ in CH_2Cl_2; the yield is 38% after recrystallization from a saturated CH_2Cl_2–hexane solution. IR (CH_2Cl_2): ν(C=C) 1608 (w) cm^{-1}; ν(CO) 1930 (s), 1835 (s) cm^{-1}. ^{1}H NMR (400 MHz, $CDCl_3$): δ 1.95 (d, 1 H, H^1), 2.75 (t, 1 H, H^4), 3.04 (m, 2 H, H^2 + H^3), 3.45 (d, 9 H, P(OCH$_3$)$_3$), 4.98 (d, 1 H, H^7), 5.21 (m, 2 H, H^5 + H^6), 6.0–7.5 (16 H, Ph, pz), J_{13} = 9.8 Hz, J_{23} = 6.4 Hz, J_{34} = 9.2 Hz, J_{45} = 10.1 Hz, J_{56} = 16.8 Hz, J_{67} = 10.2 Hz. ^{13}C NMR (100 MHz, $CDCl_3$): δ 58.6 (CH^{1}H^2), 51.8 (d, P(OCH$_3$)$_3$, 23 Hz), 77.7 (CH^4), 103.7 (CH^3), 117.0 (CH^{6}H^7), 138.5 (CH^5), 224.9 (d, Mo–CO, J_{PC} = 11 Hz), 225.2 (d, Mo–CO, J_{PC} = 11 Hz). Anal. Calcd for $MoC_{28}H_{32}O_5N_4BP$: C, 52.35; H, 5.02; N, 8.72. Found: C, 52.10; H, 5.02; N, 8.56.

(o) Synthesis of [(C$_6$H$_5$)$_2$B(OH)(pz)Mo(η^3-NNCHCHCHCH$_2$CHCHCHCH$_3$)(CO)$_2$] (7a). Complex **5a** (0.20 g, 0.38 mmol) was dissolved in THF (20 mL) containing 0.5 mL of H_2O, and the mixture was stirred for 6 h. After removal of the solvent, the residue was chromatographed through a neutral alumina column with CH_2Cl_2 as the eluting solvent. A yellow band, mainly consisting of unreacted **5a**, was eluted off the column. The top immobile brown band, after being eluted with CH_3CN, was developed into a gold-yellow band, collected, and evaporated to dryness. Further recrystallization from CH_2Cl_2–hexane produced a yellow crystalline solid of **7a** (0.059 g, 0.11 mmol). IR (Nujol): ν(CO) 1952 (s), 1870 (s) cm^{-1}. ^{1}H nMR (400 MHz, $CDCl_3$): δ 1.90 (d, 3 H, CH_3), 2.05 (dt, 1 H, H^1), 2.40 (t, 1 H, H^3), 2.65 (t, 1 H, H^2), 4.60 (dd, 1 H, H^4), 5.40 (d, 1 H, H^5), 6.0–8.2 (16 H, Ph + $C_3H_3N_2$), $J_{1\text{-}CH_3}$ = 6.4 Hz, J_{12} = J_{23} = 9.2 Hz, J_{34} = 3.4 Hz, J_{45} = 16.0 Hz. Anal. Calcd for $MoC_{25}H_{25}O_3N_4B$: C, 55.94; H, 4.67;

N, 7.83. Found: C, 55.82; H, 4.45; N, 7.72.

(p) Synthesis of $[(C_6H_5)_2B(OH)(pz)W(\eta^3\text{-}NNCHCHCHCH_2CHCHCHCH_3)(CO)_2]$ (7b). $Na(C_6H_5)_2B(pz)_2$ (0.16 g, 0.49 mmol) was added to $W(CO)_2(CH_3CN)_2(\eta^3\text{-}C_5H_7)Br$ (0.27 g, 0.50 mmol) in 50 mL of CH_2Cl_2, and the mixture was stirred at 23 °C for 30 min. The solvent was then removed in vacuo, and ^1H NMR spectra of the residues showed the presence of $[(C_6H_5)_2B(pz)_2W(CO)_2(\eta^3\text{-}C_5H_7)]$ (**5b**) and **7b**. ^1H NMR for **5b** (400 MHz, $CDCl_3$): δ 0.50 (d, 1 H, H^2), 0.60 (d, 1 H, H^6), 2.80 (m, 1 H, H^4), 5.29 (d, 1 H, H^7), 5.35 (d, 1 H, H^6), 6.20 (m, 1 H, H^5). The residue was chromatographed through a neutral alumina column, and a yellow band consisting of an unknown organic component was eluted off the column. Elution of the top immobile brown band with CH_3CN produced a gold-yellow band of **7b**. Removal of the solvent under reduced pressure gave a yellow solid, which was recrystallized from a saturated CH_2Cl_2–hexane solution to yield yellow block-shaped crystals of **7b** (0.063 g, 0.10 mmol). IR (Nujol): ν(CO) 1950 (s), 1871 (s) cm^{-1}. ^1H NMR (400 MHz, $CDCl_3$): δ 1.93 (d, 3 H, CH_3), 2.08 (dt, 1 H, H^1), 2.38 (t, 1 H, H^3), 2.65 (t, 1 H, H^2), 4.62 (dd, 1 H, H^4), 5.30 (d, 1 H, H^5), 6.0–8.2 (16 H, Ph + pz), $J_{1\text{-}CH_3}$ = 6.4 Hz, J_{12} = J_{23} = 9.2 Hz, J_{34} = 3.5 Hz, J_{45} = 15.4 Hz. Anal. Calcd for $WC_{25}H_{25}O_3N_4B$: C, 47.83; H, 3.98; N, 8.95. Found: C, 47.52; H, 3.86; N, 8.84.

(q) Solution Dynamics. A sample of **5a** was dissolved in toluene-d_8 and NMR spectra were recorded over the temperature range −60 to +90 °C. Probe temperatures were calibrated by using the temperature dependence of the differences in the chemical shifts between the ^1H resonances of the methyl and hydroxyl groups of methanol below ambient temperature and between the ^1H resonances of the methylene and hydroxyl groups of ethylene glycol above ambient temperature. Theoretical line shapes were calculated for a series of rates by using the method of Johnson.[29] Exchange rate constants for each temperature were determined by matching the theoretical spectra to experimental spectra. The rate constants k were then used to calculate the energy of activation ΔG^* at each temperature T, by using the Eyring equation:

$$k_C = (k'/\hbar)Te^{-\Delta G^*/RT}$$

k' = Boltzmann constant, $\hbar$ = Planck constant (divided by 2π), R = ideal gas constant

(r) X-ray Diffraction Study. Single crystals of **3a**, **5a**, **6a**, and **7b** were sealed in glass capillaries under an inert atmosphere. Data for **3a** were collected at room temperature on a Nicolet R3m/V diffractometer using graphite-monochromated Mo Kα radiation. The structure of **3a** was solved by the Patterson method. All data reduction and structural refinement were performed by means of the SHELXTL PLUS package. Data for **5a**, **6a**, and **7b** were collected on a Nonius CAD-4 diffractometer, using graphite-monochromated Mo Kα radiation, and the structures were solved by the Patterson method. All data reduction and structure refinement were performed with the NRCCSDP package. Crystal data and details of the data collection and structure analysis are summarized in Table V. For all four structures, all non-hydrogen atoms were refined with anisotropic parameters. All hydrogen atoms included in the structure factor calculations were placed in idealized positions.

Supplementary Material Available: Listings of bond lengths and angles, thermal parameters, and H atom positional parameters for **3a**, **5a**, **6a**, and **7b** (18 pages); listings of observed and calculated structure factors (46 pages). Ordering information is given on any current masthead page.

(29) Johnson, C. S. *Am. J. Phys.* **1967**, *35*, 928.

Tetraethylborate as an Ethyl Transfer Reagent

Eric G. Thaler and Kenneth G. Caulton*

Department of Chemistry, Indiana University, Bloomington, Indiana 47405

Received December 8, 1989

Reaction of $NaBEt_4$ with $RhCl(C_2H_4)$(triphos) (I), where triphos is $MeC(CH_2PPh_2)_3$, gives $RhH(C_2H_4)$(triphos). Coordinated $^{13}C_2H_4$ in labeled I is liberated during the reaction, proving that $NaBEt_4$ is the source of the ethylene coordinated in the product. Compound I reacts at 1 atm and 25 °C with $^{13}C_2H_4$ or H_2 to give $RhCl(^{13}C_2H_4)$(triphos) or $Rh(H)_2Cl$(triphos), respectively. It is proposed that all three reactions proceed by a mechanism in which one arm of the triphos ligand in I dissociates to yield a planar $RhCl(C_2H_4)(\eta^2$-triphos) transient. Both five-coordinate species $RhX(C_2H_4)$(triphos) (X = H, Cl) are unusual in showing relatively high barriers for both phosphorus site exchange and olefin rotation. In contrast to the reaction of I with $NaBEt_4$, the reaction with $NaBPh_4$ stops at $Rh(\eta^2$-triphos)(η^6-$PhBPh_3$) and shows no further conversion to $RhPh(C_2H_4)$(triphos).

Introduction

We have reported recently[1] on a group of Rh(III) trihydride and trimethyl compounds containing the tridentate ligand $MeC(CH_2PPh_2)_3$ ("triphos"). These 18-electron compounds were quite reactive under very mild conditions with CO, with H_2, and with ethylene. This high reactivity was traced to mechanisms that were initiated by dissociation of one arm of the triphos, a step which we initially found surprising. We report here an examination of the products and mechanisms of some reactions of a Rh(I)/triphos compound. An "arm-off" mechanism is also implicated in these reactions. This work also demonstrates an example of tetraethylborate functioning as an ethyl transfer reagent.

Experimental Section

General Procedures. Pentane, tetrahydrofuran, benzene, and toluene were all dried and distilled prior to use from solutions containing sodium/potassium benzophenone ketyl. Methylene chloride was refluxed over P_2O_5 and distilled prior to use. Sodium tetraphenylborate was purchased from Aldrich. Sodium tetraethylborate (*Caution*! pyrophoric) was purchased from Alfa. $[Rh(COD)Cl]_2$,[2] $[Rh(C_2H_4)_2Cl]_2$,[3] and RhH_3(triphos)[4] were pre-

(1) Thaler, E. G.; Folting, K.; Caulton, K. G. *J. Am. Chem. Soc.*, in press.

(2) Giordano, G.; Crabtree, R. H. *Inorg. Synth.* **1979**, *19*, 218.

0276-7333/90/2309-1871$02.50/0